Corrosion Behavior of 7075-T651 Aluminum Alloy under Different Environments

Beatriz Almeida Ferreira
beatrizalmeidaferreira@tecnico.ulisboa.pt

Instituto Superior Técnico, Universidade de Lisboa, Portugal

November 2017

Abstract

Aluminum alloys are widely used in the aeronautical industry especially in the main airframe. These alloys are susceptible to corrosion, accompanied by embrittlement, that, if left untreated, can make an aircraft unairworthy. With this in mind, the corrosion behavior of bare and anodized 7075-T651 aluminum alloy under a wet/dry cycle salt spray test in terms of loss of mechanical properties and fatigue life was studied. Between the wet and the dry period, three different washing methods were considered: nitric acid, freshwater, and no wash. The effects of corrosion on the tensile properties revealed a general decay with increasing exposure time for ultimate tensile strength and yield stress. The Young's modulus did not have a significant variation and the ductility measures decreased exponentially generally. The fatigue life was reduced drastically by the anodization and tended to decrease exponentially with corrosion as a result of premature crack initiation caused by pitting where pits are considered stress concentrations. From the surface analysis, the primary corrosion mechanism detected was pitting. The pits started to appear in random places all over the exposed surface and they coalesced, preferably in the grain direction, with neighboring pits creating bigger and deeper pits. A practical application was developed using the experimental results to characterize the corroded material and generate the necessary material properties in the FEM solver standard language. These properties can be used for any simulation in any structure made out of the 7075-T651 aluminum alloy, within the test domain.
Keywords: Aluminum Alloy 7075-T651, Salt Spray Test, Corrosion, Pitting, 7075-T651 Tensile Properties, Fatigue Life

1. Introduction

Aluminum alloys have been the main airframe materials since they started replacing wood in the late 1920's [1]. The 7075 aluminum alloy is normally applied in fuselage stringers and frames, upper wing stringers, floor beams, and seat rails and is subjected to corrosion. The corrosive action, which causes embrittlement, begins on the metal surface and moisture in the air is often sufficient to start corrosion. When an airplane structure, constructed of several metals, is exposed to corrosive environments such as exhaust gases, moisture, waste water, and spillage, necessary factors for corrosive action are present and some areas of the airplane are exposed to more corrosive contaminants than others [2]. Left untreated, corrosion can make an aircraft unairworthy in just a few years.

With this in mind, this master thesis was created, to generate a general corrosion model of this material using an autonomous underwater vehicle (AUV) that CEiiA is developing that has all his main structure made by anodized 7075-T651 aluminum alloy case study as a reference. This AUV can represent a worst case scenario for the aeronautical industry.

The corrosion behaviour of bare and anodized 7075-T651 aluminum alloy was studied through a wet/dry cycle salt spray test, with different washing methods. Then a quantification of corrosion was made based on loss of mechanical properties and fatigue life.

To have knowledge of the corrosion behavior of any material is important so that adequate materials are chosen for different situations. Knowing their operational time, maintenance and restoration processes can be scheduled and applied correctly which will help to prevent failures.

As for scientific value, the tests presented in this dissertation were never done before (at least published, based on the author's research) and it can encourage other scientists to invest more in the conditioning variation test cycles instead of continuous exposure. In reality, there are many variations of many parameters and the test has to be as accurate as possible.

2. Background

2.1. Topic Overview

In 1996, Chen *et al.*, [3], identified two types of constituent particles in the investigation of the role of microconstituents in pitting corrosion in Aluminum Alloy 2024-T3. Each type played a different role in inducing pitting corrosion, cathodic type promotes the dissolution of the matrix around it and anodic type dissolve themselves. Frankel, in 1998 [4], studied the factors that affect pitting corrosion and explained its phenomena. The relation between pitting and fatigue did not take long to realize, and in 1996 Chen, Wan *et al.*, [5], observed that fatigue cracks typically nucleated from one or two of the larger pits, and the size of the pit at which the fatigue crack nucleates is a function of stress level and load frequency. Pits were identified as crack origins in all corroded specimens also in Jones and Hoeppner, 2004 [6], study. They realized that it was not always the largest pit that formed/nucleated fatigue cracks. The combined effects of pit depth, pit surface area, and proximity to other pits were found to reduce fatigue life considerably.

To analyze environmental factors that affect fatigue life Chlistovsky *et al.*, 2007 [7] subjected specimens to fatigue testing while they were fully immersed in an aerated and recirculated 3.5 wt% NaCl simulated seawater solution. A damage analysis showed that the presence of the corrosive environment accelerated the damage accumulation rate to a greater extent than that observed in air, particularly at low stress ranges. Cavanaugh *et al.*, 2010 [8], included in his study variables like temperature, pH, $[Cl^-]$, exposure time, and orientation. Effects of these variables in affecting maximum pit depth and maximum pit diameter for high-strength aluminum alloy 7075-T651 were studied and reported and it was found that exposure time and pH, followed by temperature, were the most significant variables impacting pit depth.

The effect of anodic oxidation on fatigue performance of 7075-T6 alloy for pre-corroded and non-corroded specimens has been investigated by Cirik and Genel, 2008 [9], and the results indicate that the anodization has a tendency to decrease the fatigue performance. In 2013, Hemmouche *et al.* [10], studied the effects of some heat treatments and anodizing processes on fatigue life of aluminum alloy 2017. The result of fatigue tests showed a decrease in fatigue life of anodized specimens as compared to untreated ones that could mainly be attributed to the brittle nature of oxide layer and to the heterogeneous microstructure of the film.

Later, in 2015 [11], Dejun and Jinchun did a salt spray corrosion test on 7475 aluminum alloy bare and anodized. The results showed that the corrosion in the original sample surface is severe after salt spray corrosion, while the anodic oxide film was only slightly corroded, owing it to Al_2O_3 which prevents Cl^- to contact the base metal effectively.

2.2. Aluminum's Passivation

In the pH range of about 4 to 8.5, aluminum is passive (protected by its oxide film). Out of the passivation limits, aluminum generally corrodes in aqueous solution due to the dissolution of its oxides in acids or bases, however, sometimes, even though it is outside of the passivation zone, the film is insoluble or the oxidizing nature of the solution maintains the oxide layer [12].

At low nonoxidizing potential the metal itself, Al, is stable, this is called the immunity zone. On the passivity zone, the aluminum oxide, Al_2O_3, is stable which origins the protective layer. At low pH and high pH the aluminum ion, Al^{3+}, and the aluminate ion, AlO_2^-, respectively, are stable, which means the metal is subjected to corrosion on these areas [13].

2.3. Pitting Corrosion

Pitting is the most common form of corrosion found on aluminum and it is usually manifested by the random formation of pits [12]. Depending on their composition and environmental conditions the different alloys are affected differently. In general, the purer the alloy the higher pitting resistance it has because pitting occurs as a galvanic reaction between different elements on the alloy.

It is often the most damaging form of corrosion due to the ability of perforation through the depth of the metal which results in loss of strength properties through means of increased stress concentrations at these locations.

When the oxide layer breaks down the exposed metal gives up electrons easily and the reaction initiates tiny pits with localized chemistry supporting a rapid attack. This attack will cause the pit propagation (Figure 1).

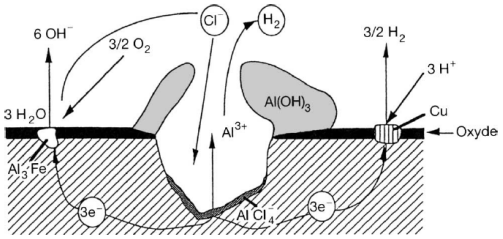

Figure 1: Mechanism of Pitting Corrosion of Aluminum (Source: [14])

Outside the cavity the reduction of water ($\frac{2}{3}O_2 + 3H_2O + 6e^- \rightarrow 6OH^-$) and of H^+ ($6H^+ + 6e^- \rightarrow 3H_2$) occurrs, which will locally lead to an alkaline pH [14].

At the pit's bottom aluminum oxidation will occur, this creates an electrical field that shifts the Cl^- ions towards the pit bottom forming aluminum chlorides. The aluminum chlorides then suffer hydrolysis forming aluminum hydroxides ($Al(OH)_3$) plus excess of hydrogen and chloride ions (H^+, Cl^-). This will lead to the acidification of the pit's bottom and the media will become very aggressive making the pit to autopropagate [14]. Because of this, pitting is considered to be an autocatalytic process which means that once it has initiated, it alters the local conditions to promote further pit growth.

$Al(OH)_3$ will precipitate and pushed to the opening of the pit where it forms a deposit of white spots [14].

2.4. Anodization

Since the aluminum has a natural protective layer, one of the methods to slow down the corrosion process is thickening that layer. This is the principle of anodization. The layer is grown by passing a direct current through an electrolytic solution, with the aluminum object serving as the anode, creating more aluminum oxide and, therefore, thickening the layer. This increases abrasion and corrosion resistance and also provides better adhesion for paints and primers [15].

3. Experimental Procedure

3.1. Specimen Description

The material used in this experiment was the Aluminum Alloy 7075-T651. The specimens were chosen in accordance with the ASTM B557M, Standard Test Method for Tension Wrought and Cast Aluminum and Magnesium Alloy Products (Metric) [16], as the Rectangular Tension Test Specimens, Standard Sheet-Type 12.5mm Wide.

The specimens were machined by an AWEA 3 axis CNC BM 1020F from $600 \times 400mm$ aluminum sheets with 3 mm in thickness. To help with vibrational issues a $600 \times 400mm$ vacuum table was used to hold down the sheet during machining.

After machining, half of the specimens were anodized according to AMS2469 which is a standard for hard anodic coating on aluminum and aluminum alloys.

The test has a total duration of 20 cycles. Five exposure times were considered (1 cycle, 3 cycles, 9 cycles, 15 cycles and 20 cycles) to obtain a more accurate tendency line of the loss of mechanical properties and fatigue life. For each time interval, thirty-six specimens were manufactured, eighteen for fatigue testing and eighteen for tensile testing. The specimens were further divided into anodized and not anodized and on the three washing methods. To get representative average values of all the parameters for each set of conditions three replicates were tested.

An addition of twelve specimens was also machined for the uncorroded tests, half for fatigue and half for tensile studies further divided into anodized and bare specimens.

With the goal of observing how S-N fatigue curves would change with increasing corrosion, an extra 15 samples were considered all not anodized and washed with freshwater. These 15 test specimens were tested at the Mechanical Testing Laboratory of Instituto Superior Técnico with the same testing conditions and procedure.

A total of 207 specimens were tested.

Before the beginning of the tests, the specimens were cleaned and the ones that will be inserted inside the salt spray chamber were masked on the grip areas with a $3M^{TM}$ Corrosion Resistant Duct Tape ($50mm \times 50m$) in order to protect these areas from corrosion.

The specimens were then labeled according to the different combinations of exposure time ('0','1', '3', '9', '15' or '20'), anodized or not ('A' or 'NA', respectively), the three washing methods ('B' - nitric acid, 'C'- freshwater and 'D'- not wash) and the replicate number ('01', '02' or '03') (e.g. 1-NA-B-02: replicate number 2 of a bare specimen washed with nitric acid exposed to one corrosion cycle).

3.2. Corrosion Test

To simulate a device that goes in seawater for a few hours and then gets stored in a warehouse during a certain period of time until it goes in seawater again, a wet/dry cycle of an 8h wet period and a 15h dry period was executed (Figure 2). These periods of time result in a total test duration of 460 hours (20 cycles).

In the wet period, the specimens were inside the salt spray chamber (ACS Dry Corrosion Test Cabinet 1200) following the ASTM B117 - Standard Practice for Operating Salt Spray (Fog) Apparatus [17] at the temperature of $35°C \pm 2°C$, with a salt solution with 5wt.% NaCl and pH between 6.5 and 7.2.

In the dry period, the specimens were inside a humidity and temperature controlled chamber (Aralab Climatic Chamber Fitoclima 500 EP20). The temperature was 25°C and the relative humidity (RH) was 80% to simulate a warehouse near the sea.

In all extracted specimens, with a MITUTOYO Surface Roughness Measuring Tester, a roughness profile was measured. From this profile, with an MS Excel Macro, designed purposely for the task, the maximum valley depth, average valley depth, and valley density were obtained. A microscopical observation (Nikon ECLIPSE MA 100) of every specimen was also performed and some photographs

(Nikon NIS Elements D software) were taken of pits, cracks and other interesting microstructures.

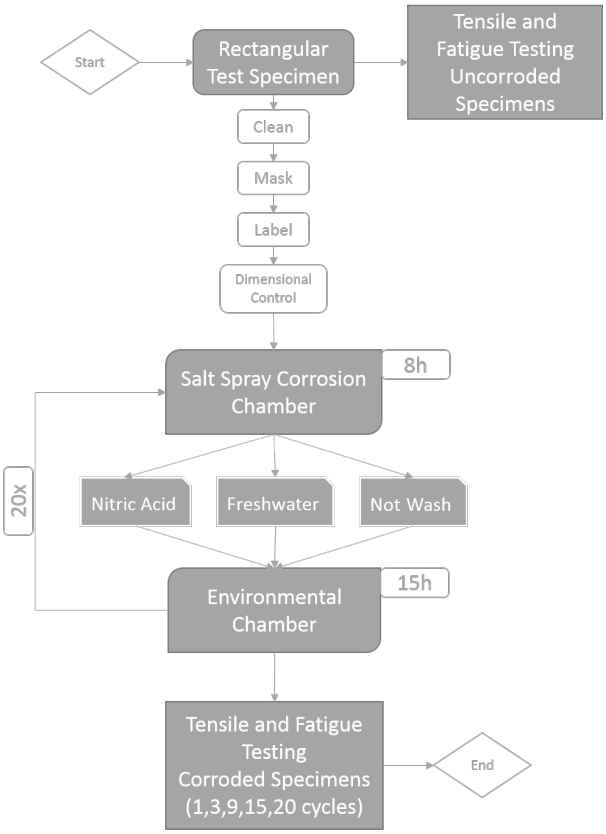

Figure 2: Scheme of the Test Procedure

3.3. Tensile Test

The test was performed following the standard ASTM B557M - Standard Test Method for Tension Wrought and Cast Aluminum and Magnesium Alloy Products (Metric) [16]. The machine used was an MTS Servohydraulic Testing Machine with a load cell of 100kN and an integrated Linear Variable Differential Transformer (LVDT) with a defined rate of displacement of 1mm/min. During the experiment, an MTS 632.85 Biaxial Extensometer was mounted on the specimens to measure axial and transverse deflections.

3.4. Fatigue Test

The test was performed following the ASTM E466 - Standard Practice for Conducting Force Controlled Constant Amplitude Axial Fatigue Tests of Metallic Materials [18].

The machine used in this experiment was the MTS Servohydraulic Testing Machine with a load cell of 50kN and an integrated LVDT. The test conditions were SR=0.1, f=10Hz and a maximum stress of 165.5MPa. The test limit is 1 million cycles. For the S-N curve specimens, the maximum stress is variable but the other conditions are the same.

4. Results

4.1. Corrosion Test Results

The surface evaluation revealed that the initiation of pits is confined to very few sites although they started to appear already on the first cycle.

The specimens washed with nitric acid (AB and NAB) were the more degraded, with the biggest and deeper pits. In the anodized case, the acid dissolved the aluminum oxide that constitutes the oxide layer, discoloring the specimens. This brutal discoloration happened after the very first wash and after that, the color continued to go back to the specimen's original color, before anodization. The initial circular pits started to merge with close neighboring pits preferably along the grain direction. A large pit found in an anodized washed with nitric acid sample, after 20 cycles of exposure, with an approximate area of 0.256 mm^2, is shown in Figure 3.

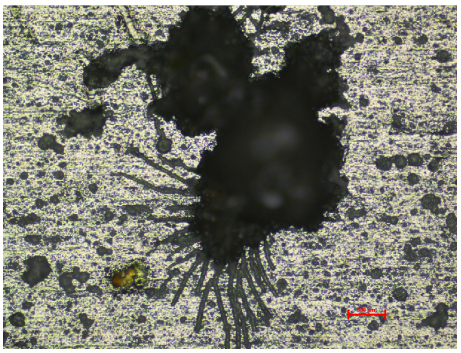

Figure 3: Microscopic Image of a 20AB Specimen

Around the perimeter of this pit, there are pit lines coming out meaning the continuous propagation of the pit. These pit lines initiated on the edges of the bigger pit and are growing outwards. This is one of the aspects that decreases fatigue life because it covers the crack initiation stage and even a little bit of the crack propagation period of the fatigue process.

In the specimens washed with freshwater, it can be seen a breakdown of the anodization layer and a small discoloration as the corrosion time increases, in the anodized samples. However, after the 20 cycles, the specimens did not present any significant damage, which means that the anodization protected the metal surface effectively. As for the not anodized samples, the crackle effect of the breakdown of the natural oxide layer became more evident. Pits appeared, with different sizes, all over the exposed surface and also coalesced with close pits. Even though these specimens were washed with freshwater they were dirty, with significant salt residues but not as much as the non-washed.

The non-washed specimens had a similar behavior to the washed with freshwater either in the anodized case or the bare case. The anodized spec-

imens did not have many salt depositions on the surface but had a small discoloration and an increased density of cracks on the layer with increase corrosion. On the bare samples, the breakdown of the oxide layer started with a fish scale pattern and then changed to a crackle effect. Pits appeared and as they grow also new ones show up.

All the samples were more corroded on the edges than on the middle part of the exposed surface.

The roughness profile analysis exhibit a general increase of maximum valley depth and average valley depth for all specimen variations and an oscillating valley density. The more corroded samples (AB and NAB) have the highest maximum and average valley depth, and the least corroded (AC and AD) have the lower values. As for the valley density, the oscillating variation is because in the beginning pits started to appear in a disperse way increasing the valley density, but after this, they started to get together making one larger pit which means that the density decreases.

4.2. Tensile Test Results

The evaluated parameters from the tensile tests were the ultimate tensile strength, yield stress, Young's modulus, elongation at fracture and reduction area.

Before corrosion, the main difference between anodized and bare specimens in terms of the mechanical properties considered are the ductility measures (elongation at fracture and reduction area). Since the anodic film is brittle the ductility is slightly less when comparing anodized with untreated specimens.

Almost all of the properties decreased with increasing corrosion exposure time as we can observe in Figure 4, the lines get lower (lowering ultimate tensile strength and yield stress) and they also get shorter (lowering the strain at fracture), the Young's modulus is practically the same (the slope of the elastic area is almost the same in all cases).

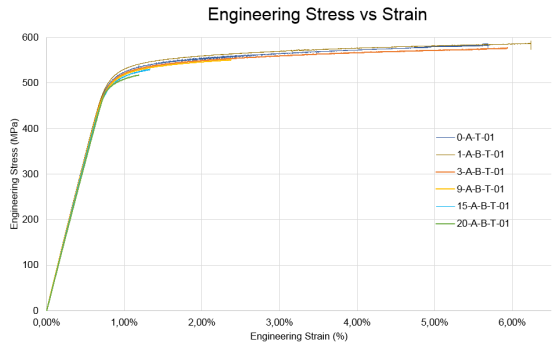

Figure 4: Engineering Stress-Strain Curve Evolution for AB Specimens

Ultimate and yield stress followed a liner decreasing trend, in general; Young's modulus did not have a significant variation; elongation at fracture and reduction area decreased exponentially to extremely low final values.

4.3. Fatigue Test Results

Due to the anodic film, there was a decrease of 91.1% in fatigue life just by anodizing the specimens.

It is generally accepted that reduction in fatigue performance of anodic oxide coated specimen is directly related to the brittle and porous nature of the coating layer and tensile residual stress induced during coating process [9]. The thicker the coating the more irregularities it contains which also contributes to the decrease in fatigue life. Increasing the thickness also causes a larger area for micro crack growth and coalescence.

For thicker oxide layers (for example hard anodization) the crack formation can also be attributed to the difference in thermal expansion coefficients between the aluminum substrate and the coating layer along with internal tensile residual stresses in the coating [9].

As for the evolution of fatigue life with increasing corrosion cycles, there was a general decreasing exponential trend. The not anodized specimens had a significant loss in fatigue life with just one cycle of exposure which means that the smallest amount of corrosion reduces a lot fatigue life. After the first cycle, the differences were not so accentuated but it still decreased.

Concerning the anodized samples, at first, since the whole corrosion process dissolves the anodic layer, there is almost a maintenance of fatigue life or even a slight increase in the first cycle. After that between the continuous dissolution of the film and simultaneous corrosion, fatigue life decreases. This is more noticeable on the specimens washed with nitric acid (AB) (due to the almost complete dissolution of the anodic layer) but it also occurs on the other anodized samples.

Even though the not anodized started with higher fatigue lifetimes after twenty cycles they ended up with less fatigue life than the anodized samples. This is because the anodization prevented the pit formation where the fatigue cracks tend to initiate from which means that pitting reduces fatigue more than anodization on its own does.

Pits are considered stress concentrations from where the failures occur. Fatigue cracks can nucleate from these corrosion pits and grow at an accelerated rate in a corrosive environment. The reduction in fatigue life present in every test specimen is primarily a result of premature crack initiation caused by pitting. The pits create an accumulation of local irreversible plastic deformation and microscopic

flaws that grow and coalesce with other flaws from other microscopic cracks.

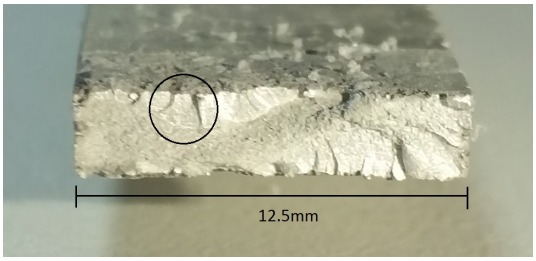

Figure 5: Specimen's Cross Section After Fatigue Test [Courtesy of CEiiA]

Figure 5 shows a cross section of a selected specimen after a fatigue test. This specimen had several initiation points. As the fatigue test runs cracks started to appear, preferably where pits were, on both of the surfaces. The circle in Figure 5 highlights two pits that got deeper along the cyclic loading. Typical fatigue benchmarks are also visible on the lighter and softer areas and then the catastrophic failure is represented by the rougher and darker area.

In Figure 6 there are three S-N curves for a different number of corrosion exposure cycles of a not anodized washed with freshwater sample, and the first observation made is that corrosion has a tendency to decrease fatigue performance.

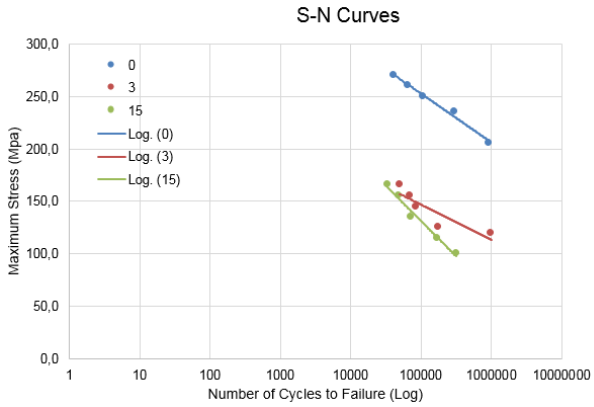

Figure 6: Effect of Corrosion on the S-N Curve of 7075-T651 Aluminum Alloy

Comparing the blue line (uncorroded specimens) with the red line (specimens that were exposed to three cycles of corrosion), it can be seen that for the same approximate interval of fatigue life the maximum stress of the cyclic load applied on the material is considerably less. The maximum stress for the approximate same amount of cycles to failure decreased around 100MPa. As for the green line (specimens that were exposed to fifteen corrosion cycles), when compared to the red line, there was a decrease in fatigue cycles for the approximate same amount of maximum stress applied. The same thing is concluded: for small amounts of corrosion big variations of fatigue life will be observed but as the corrosion exposure continues the variations start to decrease. For an increase in corrosion time, it is expected that the curve will move downwards and leftwards.

5. Finite Element Analysis

By way of comparison with the experimental results, a tensile test with a finite element model was simulated on a test specimen. After achieving similar results in both methods a practical application was created that characterizes the material based on the degradation equations found experimentally. This program uses the experimental results to characterize the corroded material and generates the necessary material properties in the finite element solver standard language. These properties can then be used for any simulation in any structure made out of 7075-T651 aluminum alloy, within the test domain.

5.1. Software

The software used for pre-processing was Altair HyperMesh, the solver was MSC Nastran and for post-processing was Altair HyperView. The 3D design of the specimen was made in CATIA by Dassault Systmes ®. The program uses a combination of MATLAB ® and MSC Nastran.

5.2. Model

Shell elements (PSHELL) with quadrilateral plate element type (CQUAD4) were used for the mesh of the specimen's geometry. After a mesh convergence study, a $3t$ mesh dimension was defined with 84 CQUAD4 elements and 1 RBE2 element. This gives a total of 117 nodes (Figure 7).

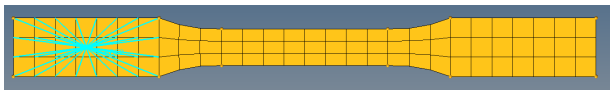

Figure 7: Meshed Specimen

Constraints are applied on the left grip of the model blocking all the degrees of freedom. A load is applied to the independent node of the RBE2 on the other grip (Figure 8).

5.3. Analysis

A linear static analysis was made in order to validate the model with the material properties of the aluminum alloy 7075-T651 uncorroded and not anodized. This analysis was made on a point from a stress-strain experimental curve. The results validated the model and are presented in Table 1.

Since the major changes occurred in the plastic part of the stress-strain curve, a material nonlin-

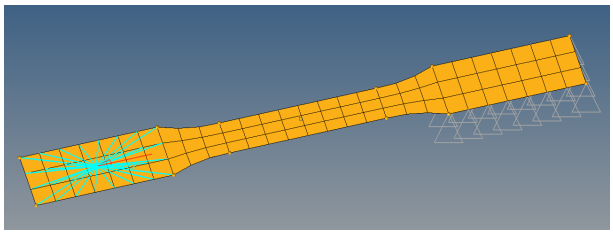

Figure 8: Load and Boundary Conditions Applied on the Specimen

Table 1: Stress and Strain Value Comparison for Linear Static Analysis

	Stress [MPa]	Strain [mm/mm]
Experimental	138.011	0.002012
Numerical	138.016	0.002012
Relative Deviation	0.004%	0.00%

earity must be considered. Therefore, a non-linear approach was also investigated.

The same elastic point was tested and the results were accurate (Table 2). A plastic point was also investigated (Table 3) and the nonlinear model was validated.

Table 2: Stress and Strain Value Comparison of a Linear Point in Nonlinear Static Analysis

	Stress [MPa]	Strain [mm/mm]
Experimental	138.011	0.002012
Numerical	138.016	0.002000
Relative Deviation	0.004%	0.06%

Table 3: Stress and Strain Value Comparison of a Nonlinear Point in Nonlinear Static Analysis

	Stress [MPa]	Strain [mm/mm]
Experimental	541.019	0.02138
Numerical	540.995	0.02131
Relative Deviation	0.004%	0.33%

5.4. Practical Application

After achieving similar results in both numerical and experimental methods a practical application was created that characterizes the material based on the degradation equations found experimentally.

When comparing the experimental tensile test curves along the exposure cycles (Figure 4) it can be observed that the slope until yield stress (the young modulus) is almost unchanged. The differences between the curves rely on the plastic part of the graph. Because of this, the curve was divided into two lines: one line from the origin to the yield stress (elastic line) and another from the yield stress until fracture (plastic line). This plasticity model is the simplest one MSC Nastran uses.

The slope of the uniaxial stress-strain curve in the plastic region is known as tangential modulus (E_T) and a linear approximation of this line can be made in the format $y = mx + b$. With the values present in the experimental tensile curves, a linear approximation of the plastic line was made for the different experimental curves. The effect of corrosion had an exponential trend on the slope (m) and a linearly decreasing trend on the y-intercept (b) for all the different combinations of bare and anodized aluminum with the three washing methods. The more corroded cases (AB and NAB) had the higher increase of m and the higher decrease of b.

Having the knowledge of how the yield stress, ultimate stress and slope and y-intercept of the plastic line degrade, the material properties for any corrosion exposure time can be achieved.

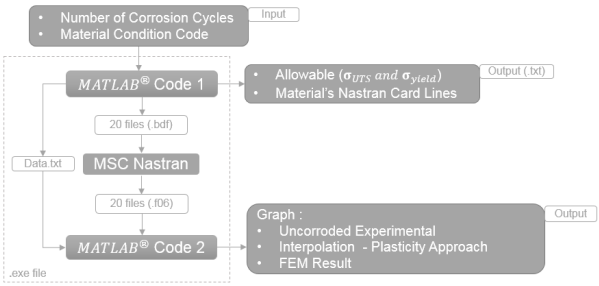

Figure 9: Program Scheme

MATLAB® code number one (Figure 9) reads the desired condition code and the number of corrosion exposure cycles and, with the formulas deduced from the experimental curves, obtains the values of yield stress, ultimate tensile strength and m and b of the material's plastic line. Inside this part of the executable, there is a pre-made Nastran card of the specimen model during a tensile test with the nonlinear analysis model. This *.bdf* file already contains all the mesh characteristics, material properties, forces, and constraints applied and default nonlinear parameters so that a nonlinear static analysis (SOL 106) can be performed.

With the ultimate stress and area values, the maximum force is calculated which is further divided into 20 force values equally spaced, so that a stress-strain curve can be constructed. After this, MATLAB® generates 20 *.bdf* files with the updated material properties (Nastran bulk data entries: MAT1, MATS1, and TABLES1) and writes, in each one, a different force value (Nastran bulk data entry: FORCE).

From this first code are also created two *.txt* files. The first file (*Output.txt*) contains the tensile strength and yield stresses of the corroded material as well as the Nastran code lines that need to be changed concerning the material properties (MAT1, MATS1 and TABLES1). The second file (*Data.txt*) contains the data from the uncorroded stress-strain

curve (contained in a vector in code one depending if the user chooses an anodized or a bare material) and the interpolated curve constructed based on the plasticity theory.

The next step is to run the 20 *.bdf* files in Nastran which generates 20 $.f06$ files. Since it is only needed one value for stress and strain, one element from the mesh had to be chosen. In tensile tests, the "dogbone" specimen shape is the most typical shape so that the deformation is confined to the narrow center region to reduce the likelihood of fracture to occur at the ends of the specimen. Because of this, in the input file, the requested outputs were only the stress and the strain present in the element in the middle of the specimen, being this region the most probable for fracture to occur.

The second MATLAB® code reads the results of the finite element analysis as well as the data from the *Data.txt* file. With this values, it plots a graph comparing three stress-strain curves: the uncorroded experimental, the interpolation based on the plasticity approach considered and the FEM result.

6. Conclusions

- Corrosion exposure to salt fog leads to extensive pitting of the not anodized material since the first cycle, as expected;
- Increased corrosion was present on the edges of the exposed surface;
- Anodization protected the metal effectively from corrosion;
- Maximum and average valley depth both increased with exposure time. Valley density had a lot of variations but with small amplitude;
- Reduced cross-section and stress concentrations caused by corrosion greatly influenced the load carrying capacity of the specimen reducing, in general, ultimate and yield stress at a constant rate;
- Corrosion-induced degradation of mechanical properties occurs gradually for every tensile condition tested. Young's modulus did not have a significant variation. Elongation at fracture and reduction area decreased exponentially to extremely low final values;
- From the tensile tests, the ductility measures were the more affected properties with higher degradation percentage. Corrosion increased the material's brittleness which in turn can change the failure mode to a much more dangerous brittle failure;
- Corrosion had a greater degradation effect on the ultimate tensile strength than on the yield stress due to the fact that corrosion affected mostly the plastic domain of the material;
- Based on experimental observations, fatigue cracks initiate from corrosion pits, as predicted;
- Fatigue performance of 7075-T651 alloy was significantly reduced by the anodic oxidation process. The degrading effect was about 91.1% reduction. This reduction can be primarily ascribed to deep micro cracks formed during the anodization process;
- Fatigue life appears to follow an exponential reduction with increasing exposure time;
- Small amounts of corrosion decrease the not anodized specimens fatigue life significantly;
- The fatigue S-N curve moved down and left with increase in corrosion cycles. This means that corrosion reduces the number of cycles to failure for the same maximum load applied;
- In a long term perspective fatigue life is more reduced by corrosion on an untreated specimen than on an anodized, which makes the treatment an advantage for long term applications;
- The freshwater washing method made a more positive difference, in general, on the not anodized than on the anodized samples;
- Specimens tend to fail on the more corroded areas either in tensile or fatigue tests as anticipated;
- In a general balance, the specimens that presented the best behavior were the anodized washed with freshwater and not washed. If they resisted the salt spray exposure they will definitely resist seawater and sea atmosphere since the test is more aggressive than reality (conservative approach);
- This results correspond to the aluminum alloy 7075-T651 and cannot be extrapolated to other alloy compositions nor other temper designations.

The following recommendations are suggested for further investigation:

- The lack of a quantitative correlation between accelerated laboratory corrosion tests and in-service corrosion attack or atmospheric corrosion tests calls for additional investigation related to corrosion of aluminum structures;
- Investigating other types of corrosion tests, for example, immersion tests may produce less damaged metal and more accurate results;

- Since the device, where the material will be used, works in high pressure environments an influence of pressure in corrosion should be further evaluated;
- Some metallographic cross sections of the anodized specimens could be prepared to analyze the loss in thickness of the oxide layer along the cycles of exposure;
- To investigate the influence of corrosion on the elastic domain the test can be repeated with more corrosion cycles and more replicates for each case scenario;
- The plasticity model used can be approached with more accuracy. Suggestion: In this thesis, just two lines are defined to describe the stress-strain curve, however, this number could be increased, especially in the plastic zone.

Acknowledgements
This research was supported by CEiiA, a Portuguese center of engineering and product development. The author acknowledges B. Albuquerque, T. Rebelo, P. Figueiredo, C. Silva, S. Sampaio, J. Torrejon, M. Oliveira and I. Martins of CEiiA and Professor L. Reis of IST, University of Lisbon.

References

[1] P Rambabu, N Eswara Prasad, and V V Kutumbarao. Aluminium Alloys for Aerospace Applications. 2017.

[2] Virginia R. Crispim and Jesse J. G. Silva. Detection of Corrosion in Aircraft Aluminum Alloys. *Applied Radiation and Isotopes*, 49(7):779–782, 1998.

[3] G. S. Chen, M. Gao, and R. P. Wei. Microconstituent-Induced Pitting Corrosion in Aluminum Alloy 2024-T3. *CORROSION*, 52(1):8–15, jan 1996.

[4] G S Frankel. Pitting Corrosion of Metals A Review of the Critical Factors. *Journal of the Electrochemical Society*, 145(6):2186–2198, 1998.

[5] G S Chen, K.-C Wan, M Gao, R P Wei, and T H Flournoy. A Transition from pitting to fatigue crack growth modeling of corrosion fatigue crack nucleation in a 2024-T3 aluminum alloy. *Materials Science and Engineering A219*, pages 126–132, 1996.

[6] Kimberli Jones and David W Hoeppner. Pit-to-crack transition in pre-corroded 7075-T6 aluminum alloy under cyclic loading. *Corrosion Science 47*, 2004.

[7] R. M. Chlistovsky, P. J. Heffernan, and D. L. DuQuesnay. Corrosion-fatigue behaviour of 7075-T651 aluminum alloy subjected to periodic overloads. *International Journal of Fatigue 29*, pages 1941–1949, 2007.

[8] M K Cavanaugh, R G Buchheit, and N Birbilis. Modeling the environmental dependence of pit growth using neural network approaches. *Corrosion Science*, 52:3070–3077, 2010.

[9] E Cirik and K Genel. Effect of anodic oxidation on fatigue performance of 7075-T6 alloy. *Surface and Coatings Technology*, 202:5190–5201, 2008.

[10] L. Hemmouche, C. Fares, and M. A. Belouchrani. Influence of heat treatments and anodization on fatigue life of 2017A alloy. *Engineering Failure Analysis*, 35:554–561, 2013.

[11] Kong Dejun and Wang Jinchun. Salt spray corrosion and electrochemical corrosion properties of anodic oxide film on 7475 aluminum alloy. *Journal of Alloys and Compounds*, 632:286–290, 2015.

[12] J.R.Davis. *Corrosion of Aluminums and Aluminum Alloys*. ASM International ®, 1999.

[13] C. A. Arriscorreta and D. W. Hoeppner. Effects of prior corrosion and stress in corrosion fatigue of aluminum alloy 7075-T6. *Corrosion*, 68:950–960, 2012.

[14] Christian Vargel. *Corrosion of Aluminum*. Elsevier, 2004.

[15] Jon Perryman. Corrosion Resistance of Aluminum. *Crane Materials International*, 2007.

[16] Standard Test Methods for Tension Testing Wrought and Cast Aluminum and Magnesium Alloy Products (Metric). Standard, American Society for Testing and Materials, 2015.

[17] Standard Practice for Operating Salt Spray (Fog) Apparatus. Standard, American Society for Testing and Materials, 2011.

[18] Standard Practice for Conducting Force Controlled Constant Amplitude Axial Fatigue Tests of Metallic Materials. Standard, American Society for Testing and Materials, 1996.